Shadow Region Imaging Algorithm with Aperture Synthesis of Multiple Scattered Waves for UWB Radars

Shouhei KIDERA*, Takuya SAKAMOTO and Toru SATO
Graduate School of Informatics, Kyoto University, Japan
Email:kidera@aso.cce.i.kyoto-u.ac.jp

1 Introduction

Ultra-wide band (UWB) pulse radars are promising as near field sensing techniques with high range resolution. It is applicable to non-contact measurement of precision devices with specular surfaces, or security systems that can identify a human body in invisible situations. For these applications, the SAR (Synthetic Aperture Radar) algorithm is still promising, which can creates a stable and accurate target image even in the near field [1]. However, in the case of complex or multiple targets, this algorithm suffers from increased shadow regions or false images caused by multiple scattered waves. In most case, a multiple scattered wave propagates a different path from that passed through by a single scattered one. This means that the multiple scattered echo has independent information on target surfaces, and a potential to improve the image quality of the conventional methods, which only use single scattered waves. Although several time reversal algorithms with multiple scattered waves have been proposed, aiming at a target detection or positioning in cluttered situations [2-4], they require a target modeling or a priori information of surrounding environment like walls. To relax these conditions, this paper proposes a direct imaging algorithm based on the aperture synthesis of multiple scattered echoes. As a novelty of this paper, the proposed method is applicable to arbitrary target shapes, and directly enlarges a visible range on target surface. Some results in numerical simulation verify the effectiveness of the proposed method.

2 System Model

Fig. 1 illustrates the system model. It assumes that a target has high conductivity like metal and an arbitrary shape with a clear boundary. The propagation speed of the radio wave c is assumed as known constant. An omni-directional antenna is scanned along the x-axis. We use a mono-cycle pulse as the transmitting current. The real space in which the target and antenna are located is expressed by the parameters $\boldsymbol{r} = (x, z)$. The parameters are normalized by λ, which is the central wavelength of the pulse. $s(X, Z)$ is defined as the output of the Wiener filter at the antenna location $(x, z) = (X, 0)$, where $Z = \mathrm{c}t/(2\lambda)$ is expressed by the time t.

3 Conventional Algorithm

The SAR algorithm can create a stable and accurate target image even in the near field. The distribution image $I_1(\boldsymbol{r})$ with this algorithm is calculated as

$$I_1(\boldsymbol{r}) = \int_{X \in \Gamma} s\left(X, \sqrt{(x-X)^2 + z^2}\right) \mathrm{d}X, \tag{1}$$

where Γ is the scanning range of the antenna. The target boundary can be extracted from its focused image $I_1(\boldsymbol{r})$. Here, we show the two examples of this method in the case of complex and multiple targets as follows. The left and right hand side of Fig. 2 illustrates the outputs of the Wiener filter from the complex and multiple targets, respectively, where each signal is received at 101 locations for $-2.5 \leq X \leq 2.5$. The conductivity of each target is set to 1.0×10^6 S/m. The left and right hand side of Fig. 3 show the images obtained by the conventional method for each target case. Each image is normalized by the maximum value of $I_1(\boldsymbol{r})$. The left hand side of Fig. 3 shows that the obtained image $I_1(\boldsymbol{r})$ expresses only sharp edges on triangle boundaries, and does not obtain a most part of the target surface that falls into a shadow region. The right hand side of Fig. 3 also shows a difficulty in imaging the side of the rectangular target. This is because each antenna does not receive a direct reflection echoes from the side of target boundary which has a large inclination. This is an inherent problem in the imaging algorithms, which only use the single scattered echoes for a target reconstruction.

4 Proposed Algorithm

To overcome the problem described in the previous section, this paper proposes a shadow region imaging algorithm based on the aperture synthesis of double scattered echoes. In most case, a double scattered wave propagates a different path from that in a single scattered one, and this wave often includes an significant information of two reflection points on target boundaries. Then, a suitable use of these echoes is promising as shadow region imaging. This method calculates the image with double scattered waves by using the initial image $I_1(\boldsymbol{r})$ as

$$I_2(\boldsymbol{r}) = -\int_{\boldsymbol{r'}\in R}\int_{X\in\Gamma} I_1(\boldsymbol{r}')s\left(X, d(\boldsymbol{r},\boldsymbol{r}',X)\right)\mathrm{d}X\mathrm{d}x'\mathrm{d}z', \tag{2}$$

where $\boldsymbol{r'} = (x', z')$ is defined, R is the region of the real space, and $d(\boldsymbol{r},\boldsymbol{r'},X) = \sqrt{(x-X)^2+z^2}+\sqrt{(x'-X)^2+z'^2}+\sqrt{(x-x')^2+(z-z')^2}$ holds. The minus sign in Eq. (2) creates a positive image focused by double scattered waves, that have an inverse phase relationship from single scattered ones. Eq.(2) expresses the aperture synthesis of the received signals by only considering a double scattered path. Here, we assume that only the positive images of $I_1(\boldsymbol{r})$ and $I_2(\boldsymbol{r})$ are necessary for the target boundary extraction. Then, the proposed method determines the final image $I(\boldsymbol{r})$ as,

$$I(\boldsymbol{r}) = I_1(\boldsymbol{r})H\left(I_1(\boldsymbol{r})\right) + I_2(\boldsymbol{r})H\left(I_2(\boldsymbol{r})\right) \tag{3}$$

where $H(x)$ is defined as

$$H(x) = \begin{cases} 1 & (x \geq 0)\ , \\ 0 & (x < 0)\ . \end{cases} \tag{4}$$

The proposed method uses only the initial image $I_1(\boldsymbol{r})$ and directly emphasizes the target regions, which double scattered waves pass through.

5 Performance Evaluation in Numerical Simulation

This section shows the examples of the proposed method. The left hand side of Fig. 4 shows the image $I(\boldsymbol{r})$ for the complex target, where the same data as in the left hand side of Fig. 2 is used. This figure shows that the side of the target can be reconstructed with the proposed method, and it produces a significant image to determine the triangular boundary. Furthermore, the right hand side of Fig. 4 shows the image $I(\boldsymbol{r})$ for the multiple objects with the data as in the right hand side of Fig. 2. This figure verifies that the side region of the rectangular target is clearly stood out, and the visible ranges of circle and rectangular boundaries are remarkably enlarged. This is because the several double scattered waves are effectively focused on the target side by Eq. (2), and the region around the either of double scattered points is visible in the initial image $I_1(\boldsymbol{r})$. Moreover, it is noteworthy that this method does not require a target modeling or a priori information of surroundings, and is a significant advantage from the conventional algorithms [2-4]. We also confirm that the image obtained by the proposed method holds an accurate image in noisy situation, where S/N of the double scattered signal is more than 20 dB. However, the false images around the backside of targets appear in each example, and they should be suppressed in the future work. In addition, this method requires the triple integration of the received signals in Eq. (2), and it requires around 30 minutes for the calculation. Then, the acceleration of the imaging speed is also required for the extension to the 3-dimensional problem.

6 Conclusion

This paper proposed the direct shadow region imaging algorithm based on the aperture synthesis for the double scattered waves. In the conventional SAR algorithm, a most part of the complex or multiple targets falls into shadow region because it uses only single scattered waves. To overcome this problem, we extended the SAR algorithm with double scattered waves. The results in numerical simulation verify that this method makes visible the shadow region, and remarkably enlarges the imaging range without a priori information of target models or surroundings. Although the proposed method requires a large amount of calculation, it has a great potential to expand the application range of the near field radar in cluttered situations.

References

[1] D. L. Mensa, G. Heidbreder and G. Wade, *IEEE Trans. Nuclear Science.*, vol. 27, no. 2, pp. 989–998, Apr, 1980.

[2] S. K. Lehmanm and A. J. Devaney, *Acoust. Soc. Am.,* 113 (5), May, 2003.

[3] J. M. F. Moura, and Y. Jin, *IEEE Trans. on Signal Process.*, vol. 55, no. 1, pp. 187–201, Jan, 2007.

[4] T. Kitamura, T. Sakamoto and T. Sato, *IEICE General Conference*, C-1-9, Mar, 2008 (in Japanese).

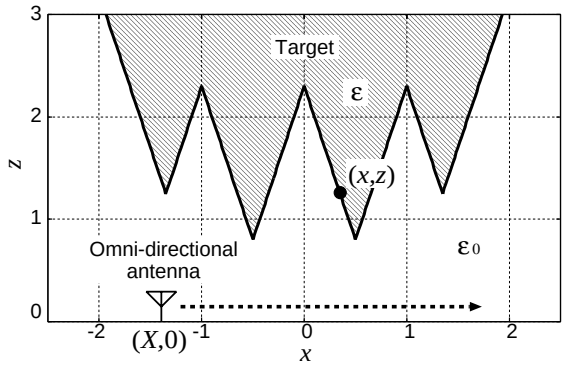

Figure 1: System model.

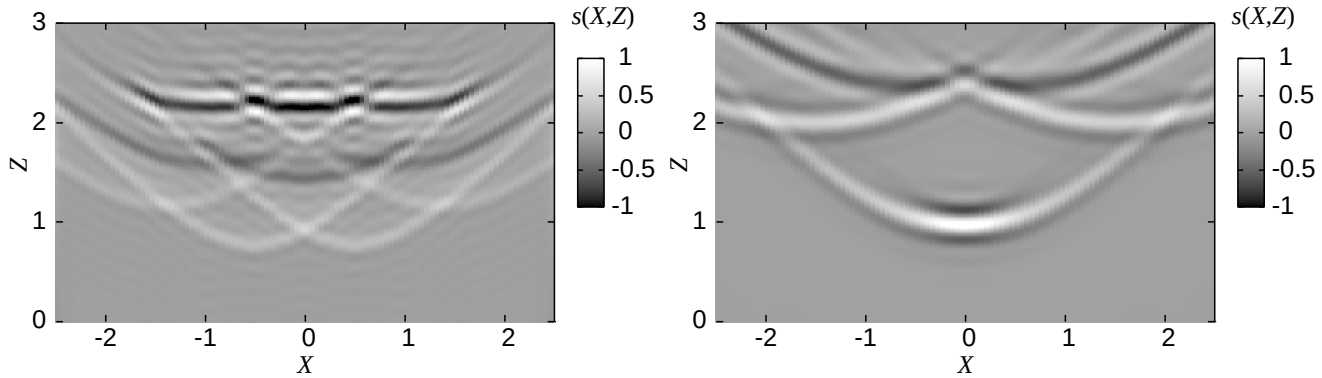

Figure 2: Outputs of Wiener filter from complex target (left) and multiple targets (right).

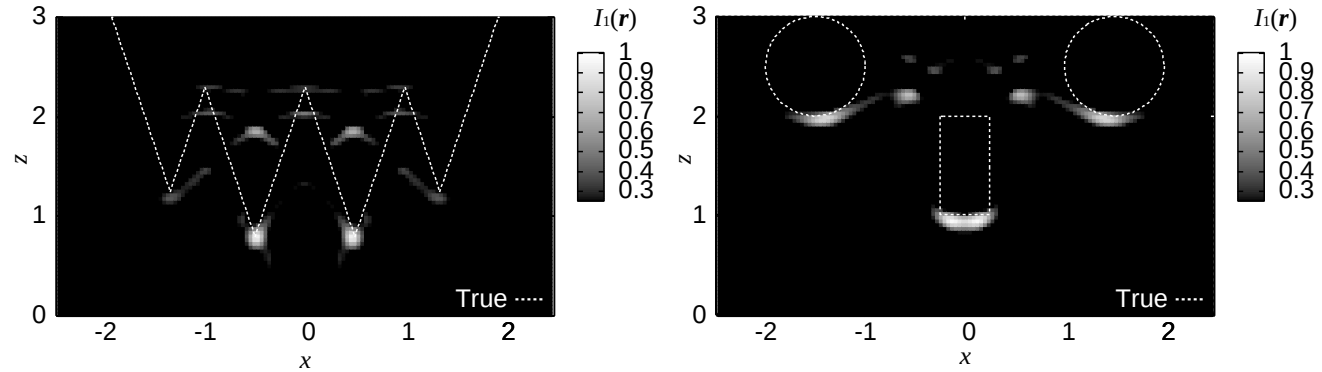

Figure 3: Estimated images with the conventional method for complex target (left) and multiple targets (right).

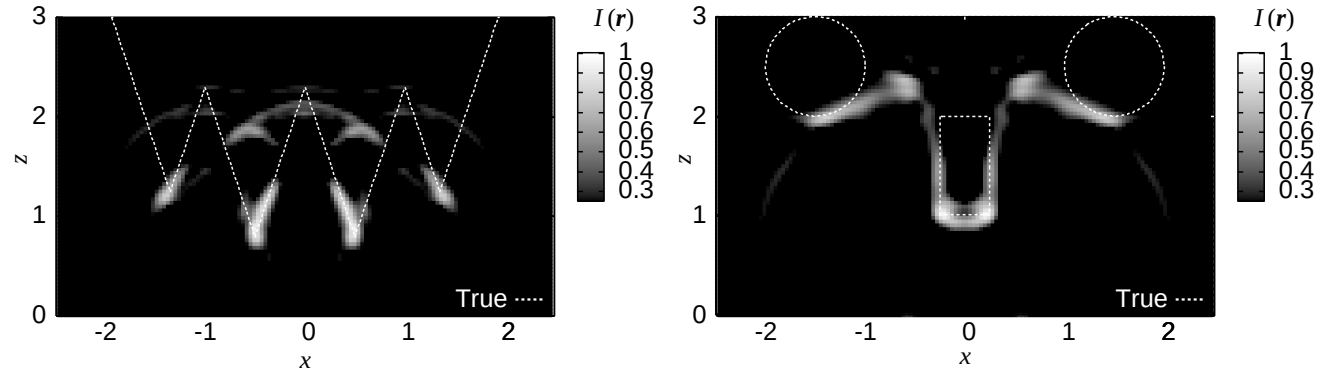

Figure 4: Estimated images with the proposed method for complex target (left) and multiple targets (right).